RESEARCH PAPER

Role of Silicon Nanocomposites for Advanced Electrical and Structural Properties: Synthesis, Characterization, Performance and Applications

Hussein Ali Hadi*, Sameer H. Al-nesrawy, Shurooq S. Al-Abbas

Department of Physics, University of Babylon, Babylon, Iraq

ARTICLE INFO

Article History:
Received 18 November 2025
Accepted 06 February 2026
Published 01 April 2026

Keywords:
Antibacterial
Electrical properties
Nanocomposite
Structural properties

ABSTRACT

Research in this area aims to create PMMA-PEO/Si nanocomposites with different concentrations of silicon (0.4, 1.4, 2.8, 4.2, and 5.6 weight percent). We suggested the nanocomposites' electrical, structural, and FTIR characteristics. The frequency, dielectric constant, and electrical loss were all reduced by applying an electric field. The results demonstrated that the electrical Loss and dielectric constant of all specimens rose as silicon levels rose. The conductivity of alternating current showed this characteristic. The researchers also collected nanocomposites made of (PMMA-PEO/Si). As the concentration of Si nanoparticles in these composites grew, they demonstrated an increasing capacity to suppress bacterial growth. Due to their unique combination of silicon's electrical characteristics with those of PMMA and PEO polymers, the findings demonstrated that the laboratory-prepared nanocomposites exhibit distinctive features. Staphylococcus, Klebsiella pneumoniae, and antibiotic-resistant bacteria were among the pathogens whose growth was efficiently inhibited by these nanocomposites in laboratory testing. These findings suggest that the nanocomposites used in this study have the potential to be useful materials in many medical contexts, particularly for the creation of new antibacterial substances that may combat the increasing problems caused by bacteria that are resistant to antibiotics.

How to cite this article
Hadi H., Al-nesrawy S., Al-Abbas S. Role of Silicon Nanocomposites for Advanced Electrical and Structural Properties: Synthesis, Characterization, Performance and Applications. J Nanostruct, 2026; 16(2):1508-1518. DOI: 10.22052/JNS.2026.02.002

INTRODUCTION

Nanotechnology encompasses the development and use of nanocomposites, offering innovative methods and commercial prospects across multiple industries, such as automotive, aerospace, superconductors, electronics, and physical and chemical fields with dimensions spanning from individual molecules or atoms to submicron scales [1-4] with sizes spanning from individual atoms and molecules to submicron dimensions. Nanotechnology is often considered the next industrial revolution [6,7]. Nanocomposite polymers, including organic polymers and nanoscale inorganic nanoparticles, are advanced materials that have attracted significant interest in recent years [8,9]. These

** Corresponding Author Email: lyh026967@gmail.com*

composite materials differ from pure polymers in both chemical and physical properties [10,11]. This may be important and advantageous for several candidates across multiple applications [12,13]. Incorporating nanoparticles into a polymer matrix may significantly improve the material's optical characteristics with low amounts of the Nanoparticles. When added to polymers, nanoparticles are better than regular additives because they don't need to be loaded as much, and they have a big effect on the physical properties. One benefit of nanoparticles as polymer additives, in contrast to traditional additives, is that their loading requirements are quite low [10] Understanding their optical behaviour is crucial for examining electronic transitions and the potential use of polymers as optical filters. Data on the electrical properties of amorphous and crystalline semiconductors is often obtained by studying their optical features over broad frequency ranges. [4]. Polymethyl a linear thermoplastic polymer known as methacrylate (PMMA). It holds melting point

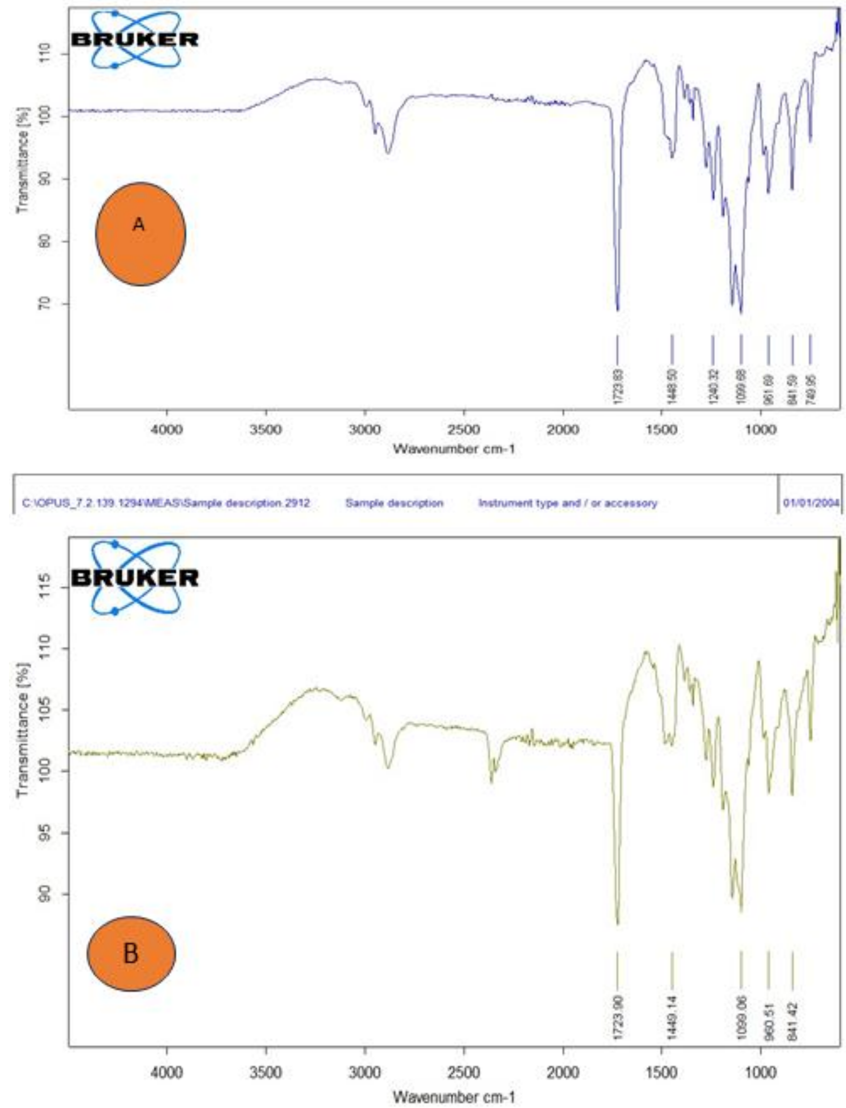

Fig. 1. IR spectra (pmma-peo/Si) complex materials: (A) for blend, (B) 1.4 wt.%.

of of160°C with a glass transition temperature of 115°C [14] PMMA has exceptional material properties, including notable mechanical strength, hardness, high rigidity, transparency, and efficient insulating capabilities [15-17].

The only drawback of PEO in applications is its insufficient optical and electrical performance at temperatures beyond its melting point. To augment its attributes [18]. PEO nanocomposite structures, including nanoparticles, exhibit robust interactions with surface functional groupings, enhancing thermal stability beyond the melting temperature of the nanocomposite [19]. Various nanocomposites may be included in PEO polymer to improve its properties and facilitate its use in multiple fields [20-25]. PEO has shown efficacy in several applications due to its unique chemical properties. Silicon is ranked the second prevalent component of our planet, exceeded only in the presence of oxygen [26-28]. Being both cheap and plentiful, it has quickly become one of the most accessible inorganic compounds. One of silicon's most common uses in the latest innovations in energy storage technology is in the semiconductor sector, which has grown exponentially in the last few decades, demonstrating the material's critical relevance. Characteristics, particularly purity and homogeneity. The top-down methodology involves the disintegration of convert mass silicon from nanostructures. Which has intensified the demand for effective, resistance-free, cost-effective, and biocompatible antimicrobial agents. Nanomaterials offer an innovative alternative to antibiotics. For example, nanoparticles have been employed to mitigate skin diseases and prevent microbial colonization on devices such as endotracheal tubes, catheters, and prostheses. Silicone derivatives combined with polymers have been utilized as anti-corrosion and chemical-resistant coatings that impede bacterial proliferation [29-32].

MATERIALS AND METHODS

The casting procedure was used to create the (PMMA-PEO/Si) nanocomposite. At room temperature, 1 gramme of (PMMA-PEO) and Si were dissolved in 50 millilitres of chloroform alcohol using a magnetic stirrer to thoroughly mix and dissolve the material. The weight ratios of Si nanoparticles added to PMMA-PEO were (1.4,2.8,4.2, and 5.6%) Using a 10-centimeter-diameter Petri dish as a mound, pouring the liquid in, waiting for it to dry, and then carefully removing it for testing is the casting procedure.

RESULTS AND DISCUSSION

FTIR spectra of (PMMA/PEO/Si) nanocomposites

Fig. 1 illustrates the various peaks in the infrared spectra of the (PMMA-PEO/Si) nanocomposites at distinct concentrations (pure, 1.4 wt%) of (Si), within the region of (4000 – 500) cm^{-1}. Fig. 1a shows the infrared spectra of (PMMA-PEO/Si), exhibiting a significant peak at about (1723.83) cm^{-1}, indicative of carbonyl (C=O) stretching, principally reflecting the interaction between PMMA and PEO. The bending vibration of (CH_2) is seen at 1448.50 cm^{-1}, while (C-O) group vibrations that stretch are noted at 1099.68 cm^{-1}. Fig. 1b displays several peaks at 1449.14 cm^{-1} and 1099.33 cm^{-1}, corresponding to (C-H) and (C-O) bonds, respectively. The observed signal at 1723.30 cm^{-1} pertains to the group of carbon atoms (C=O). At its highest point at 1099.06 cm^{-1} corresponds to the (C-O) expansion of the carbonyl group in PMMA. The (C-H) bending transpires at 960.51 cm^{-1}, outside the absorption plane of the rings. FT-IR readings indicate the absence of any chemical reaction. Where physical linkages are evident and studies concrete [33-36].

Field-emission scanning electron microscope (FESEM)

The arrangement of silicon (Si nanoparticles) within the polymer is examined through field-emission scanning electron microscopy (FESEM), and the influence of these particles on the nanocomposites is assessed. Fig. 2 present FESEM images of films derived from PMMA-PEO/Si nanocomposites, exhibiting different concentrations of Si nanoparticles. The Incorporation of silicon (Si nanoparticles) within the polymer matrix was analyzed using field-emission scanning electron microscopy (FESEM), and the effects of these particles on the properties of the nanocomposites were assessed. Fig. 2 presents FESEM images of films derived from PMMA-PEO/Si nanocomposites, showcasing varying concentrations of Si nanoparticles. Fig. 2a demonstrates the cohesiveness and homogeneity of the polymer, showing that the addition of Si nanoparticles to the PMMA-PEO polymer modifies the surface structure of the system, as evidenced by images B, C, D, and E in the figure. The average grain sizes derived from the FESEM images were 54.514 nm, 42.39 nm, 39.43 nm, and 38.60 nm for Si nanoparticles at concentrations of 1.4%, 2.8%, 4.2%, and 5.6%, respectively. FESEM images demonstrate a reduction in average grain size of 2.8% and 4.2% upon the incorporation of silicon nanoparticles, this is consistent with the researchers' findings [37].

The A.C. Electrical Properties of (PMMA-PEO /Si) Nanocomposites

Dielectric constant (ε') and dielectric loss (ε'') of (PMMA-PEO /Si) Nanocomposites

Figs. 3 and 4 illustrate that the dielectric constant and dielectric loss vary with frequency for nanocomposites composed of (PMMA-PEO/

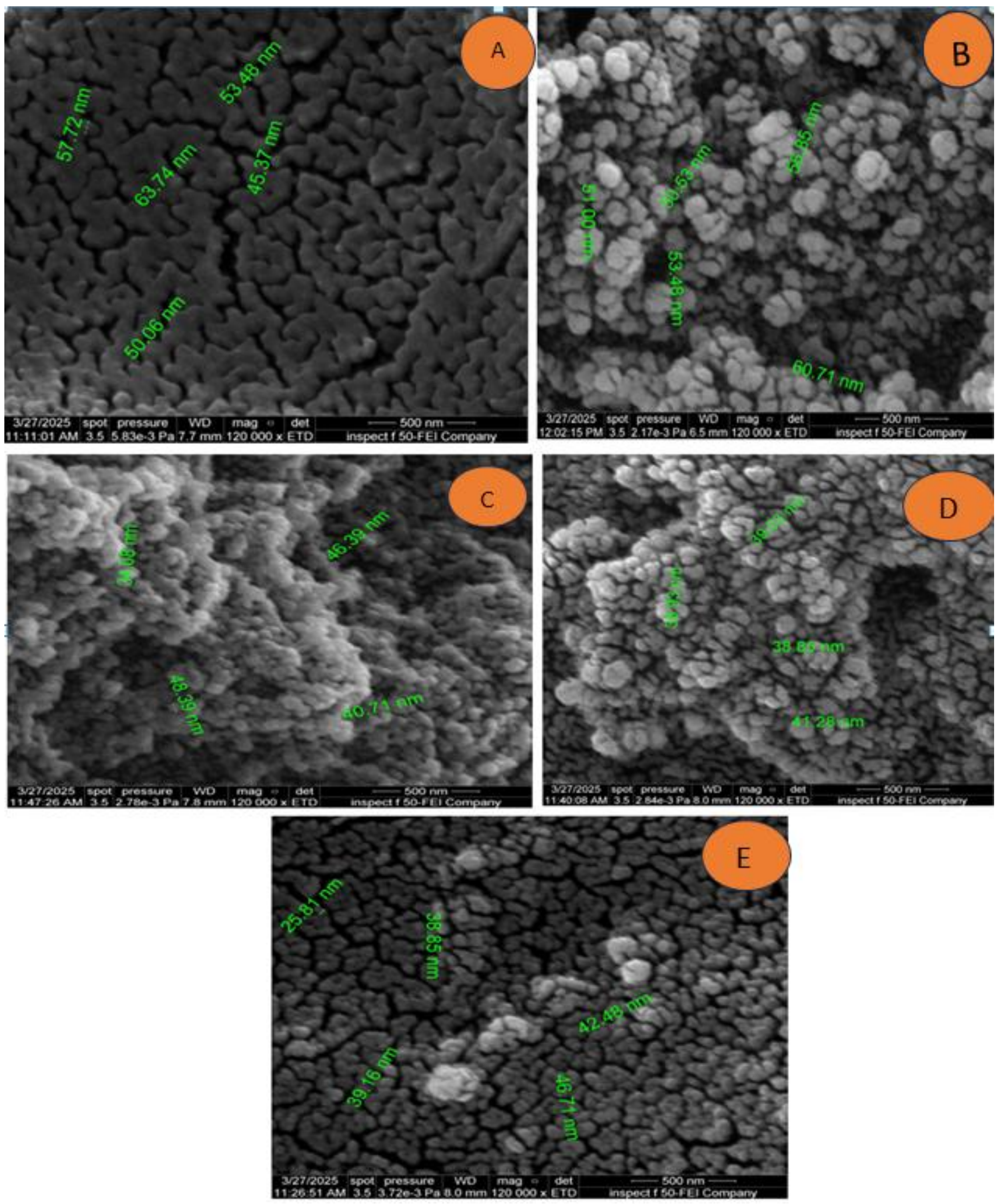

Fig. 2. The FESEM of PMMA - PEO/Si complex materials: (a) of (PMMA-PEO), (b) of 1.4 wt.% Si , (c) of 2.8wt.% Si , (d) of 4.2 wt.% Si and e) of 5.6 wt.% Si.

Si). The photos demonstrate that Maxwell-Wagner polarization leads to increased dielectric constants and losses at low frequencies. However, when the frequency escalates, these values diminish across all samples. The interaction between insulators and conductors generates this polarization. The accumulation of dipoles or space charges at interfaces leads to polarization on those surfaces. As the frequency of the applied electric field decreases, the response time of the space charges lengthens. However, the polarization effect decreases when the electric field oscillates rapidly within the higher frequency range. The dielectric loss and dielectric constant decrease with increasing frequency. This behavior corroborates the researchers' results [34].

Figs. 5 and 6 depict the relationship between the dielectric constant and dielectric loss as a function of the density of (PMM-PEO/Si) nanoparticles at ambient temperature and (100) Hz. We calculate the dielectric constant and dielectric loss of PMM-PEO/Si using the equations (ε' = Cp/Co) and (ε'' = ε›D). Darker and smaller areas indicate a reduced concentration of (PMM-PEO/Si) nanoparticles.

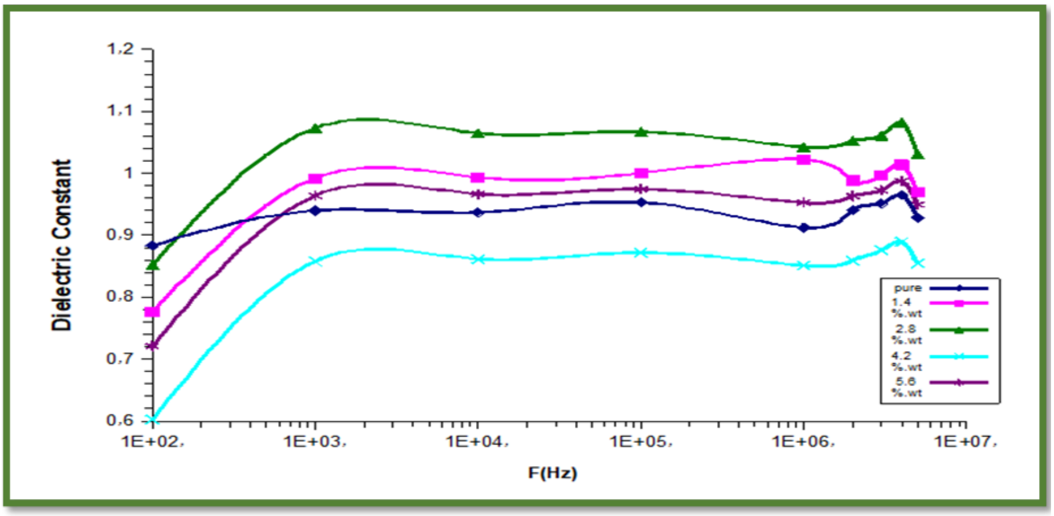

Fig. 3. Behavior of dielectric constant against frequency for (PMMA-PEO /Si) nanocomposites.

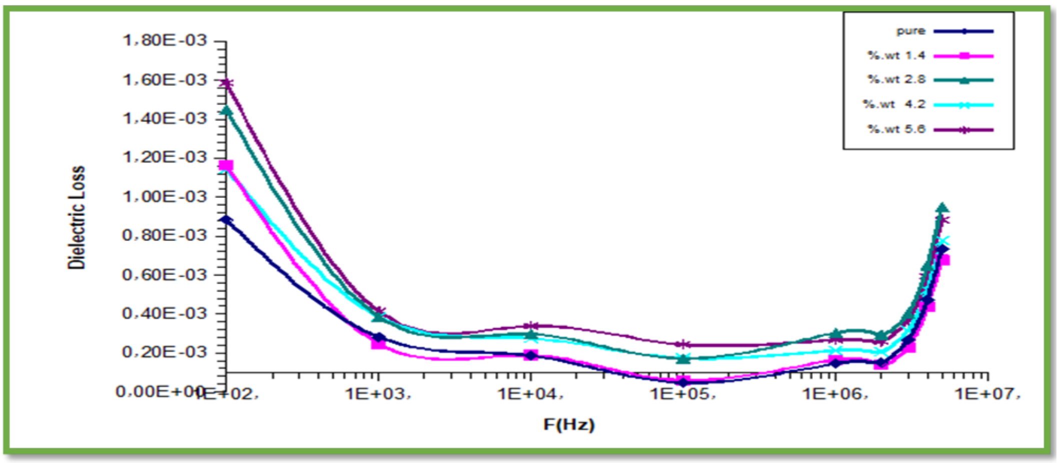

Fig. 4. Behavior of dielectric loss of (PMMA - PEO /Si) nanocomposites against frequency.

These patches form at a concentration similar to that of PMM-PEO/Si nanoparticles. The network will have overlapping paths that interlink some locations with many nanoparticles, enhancing the mobility of charge carriers. As the density of (PMM-PEO/Si) nanoparticles increases, both the dielectric constant and dielectric loss grow, attributed to the enhanced number of free charge carriers and polarization charges. This discovery aligns with [34,35].

A.C Electrical conductivity of (PMMA-PEO /Si) nanocomposites

The A.C. conductivity of nanocomposites is calculated by using the equation ($\sigma A.C = \omega \mathcal{E}o \mathcal{E}''$). Fig. 7 for a visual representation of the (PMMA-PEO/Si) nanocomposites' varying AC electrical conductivity. The relationship between this fluctuation and the room temperature electric field frequency is shown. Alternating current has a higher electrical conductivity at higher frequencies, as seen in the picture. This is due to the fact that an increase in conductivity is caused by space charge polarization [36]. Two factors that play a role in thisphenomena are the polarization of space charges at low frequencies and the enhancement of charge carriers to higher conduction band states [37,38]. Conductivity improves with increasing frequency due to electronic polarization and the mobility of charge carriers. Two variables

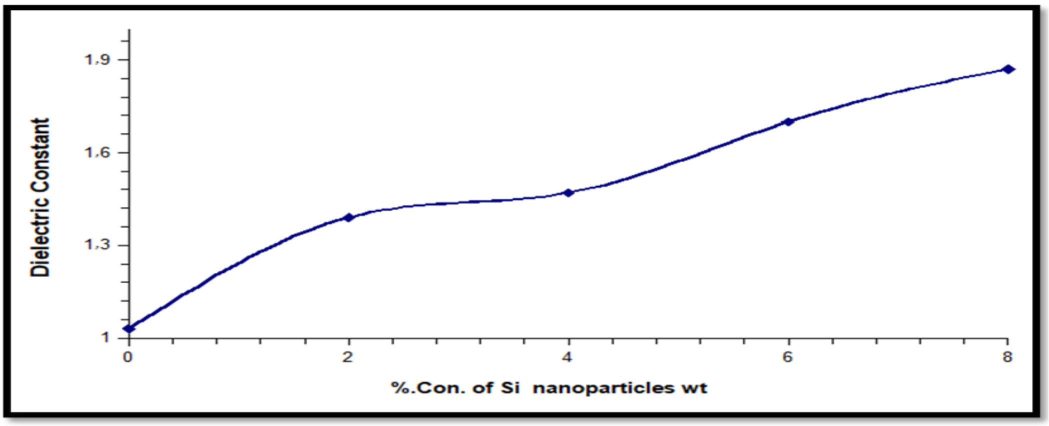

Fig. 5. Effect of (Si) nanoparticle concentrations on the dielectric constant of PMMA/PEO.

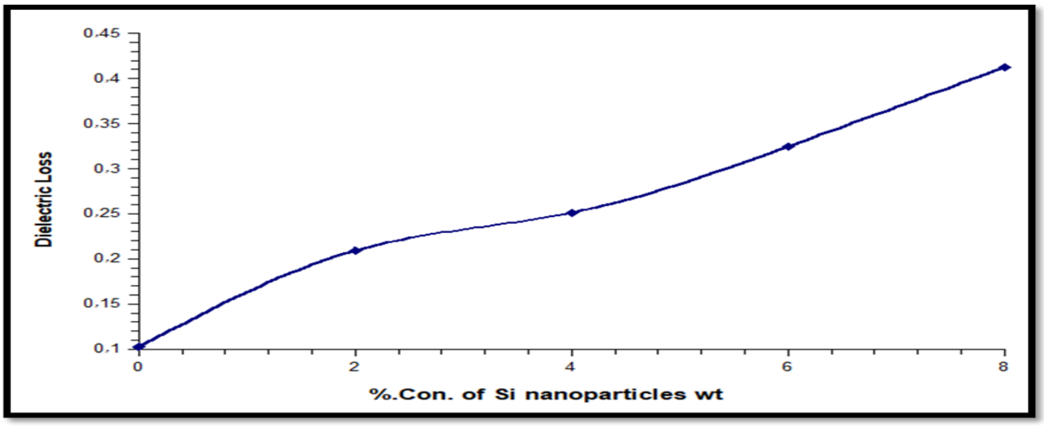

Fig. 6. Effect of (Si) nanoparticle concentrations on the dielectric of PMMA/PEO.

that influence alternating current's conducting capacity are the main chain's velocity and the passage of ions. Using a frequency of 100 hertz, Fig. 8 shows how the electrical conductivity of the PEO-PMMA mix is affected by the quantity of Si nanoparticles. Elevated alternating current electrical conductivity is a result of an increase in the charge carrier density inside the polymer

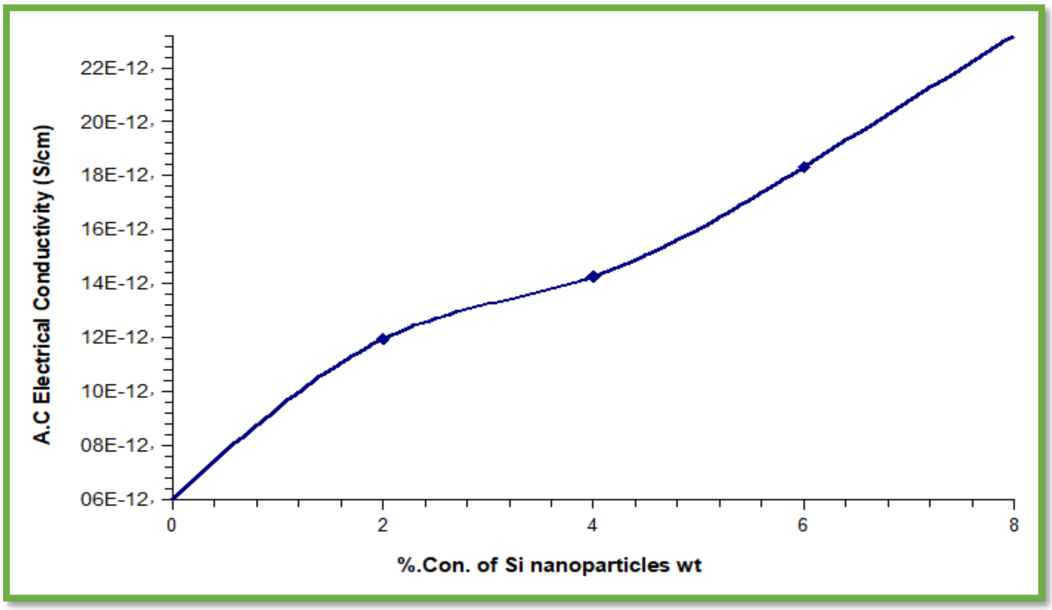

Fig. 7. Effect of (Si) nanoparticle concentrations on A.C electrical conductivity of PMMA – PEO.

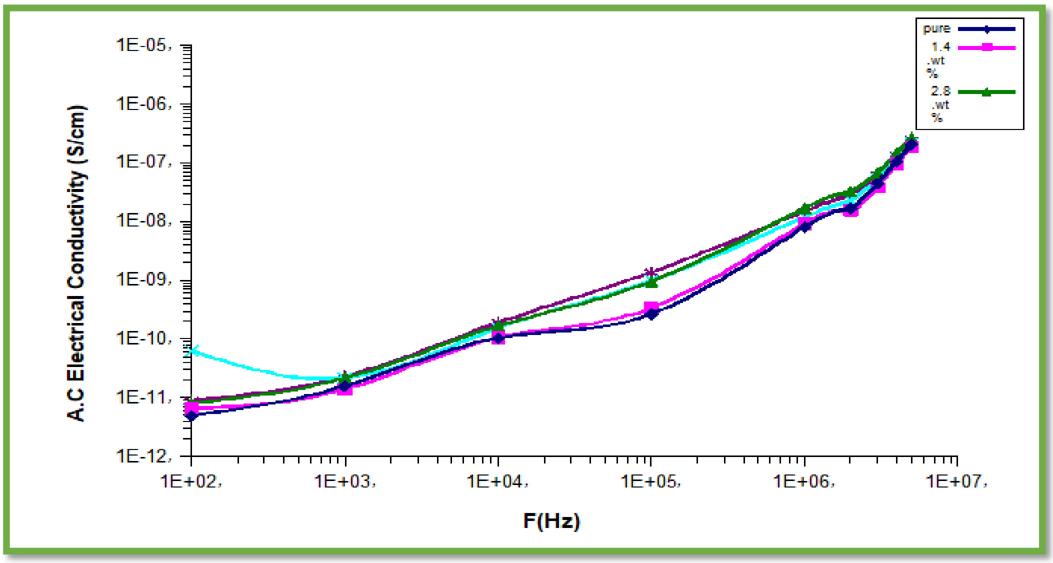

Fig. 8. Relation between A.C electrical conductivity with frequency for (PMMA-PEO /Si) nanocomposites.

medium, which is caused by the concentration of Si nanoparticles[39,40].

Application of (PMMA-PEG/Si) Nanocomposites for Antibacterial Activity

A graphic depiction of the inhibitory zones for Staphylococcus and Klebsiella pneumoniae is presented in Fig. 9. The antibacterial efficacy of nanocomposites made from polymethyl methacrylate (PMMA). The efficacy of polyethylene oxide (PEO) and silicon (Si) was evaluated against both gram-positive bacteria (Staphylococcus aureus) and gram-negative microorganisms (Klebsiella pneumoniae). The data indicate that the width of the inhibitory zones rises with the density of Si nanoparticles [34]. The rise is from 0 mm to 23 mm for Klebsiella pneumoniae and from 0 mm to 24 mm for Staphylococcus aureus in the PMMA-PEO/Si. The efficacy of the nanocomposites as antibacterial agents may be

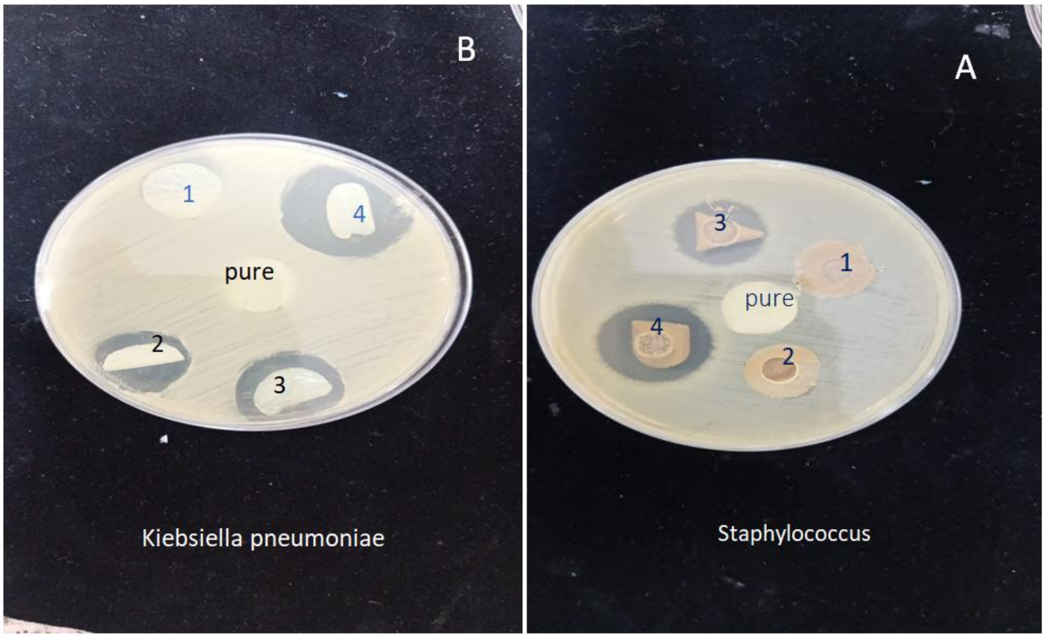

Fig. 9.)A) Images of the inhibition zone for Staphylococcus. (B) Images of the inhibition zone for Klebsiella pneumoniae.

Table 1. inhibition zone diameter of (PMMA-PEO/Si) nanocomposites.

Concentrations (Si) wt%	Inhibitions zone diameter(mm) of Staphylococcus	Inhibitions zone diameter(mm) of Klebsiella pneumoniae
Pure	0	0
1.4	15	12
2.8	18	17
4.2	21	22
5.6	23	24

ascribed to the generation of reactive oxygen species (ROS) by various nanoparticle compounds. The oxidative stress induced by reactive oxygen species (ROS) may be the primary mechanism behind the antibacterial activity of nanoparticle-based nanocomposites. A variety of radicals are included by reactive oxygen species (ROS). These radicals comprise there exist four categories of

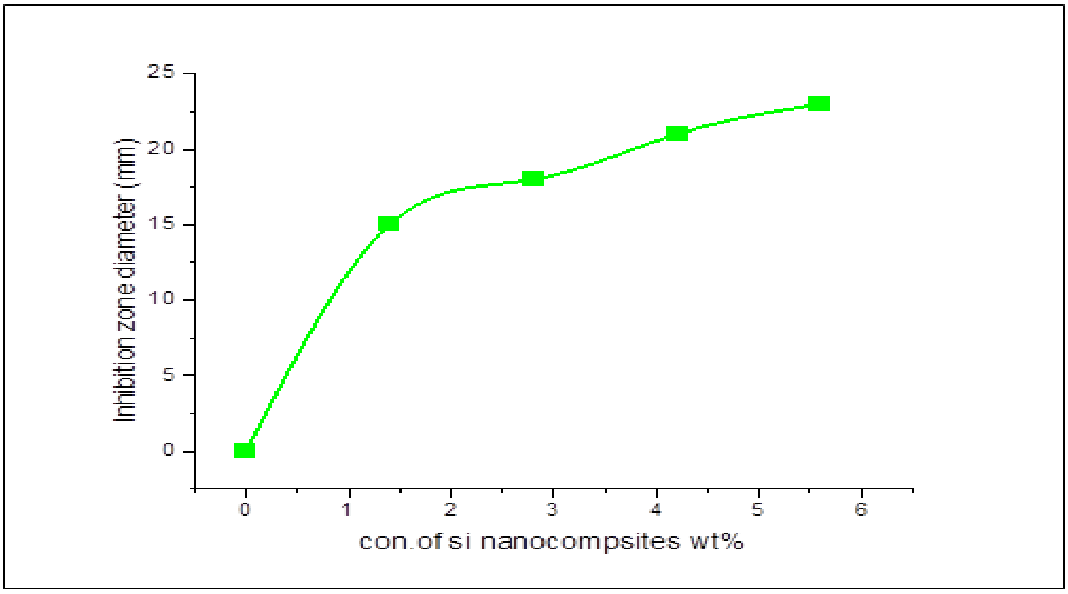

Fig. 10. Inhibition zone diameter of (PMMA-PEG/Si) nanocomposites against Staphylococcus bacterial.

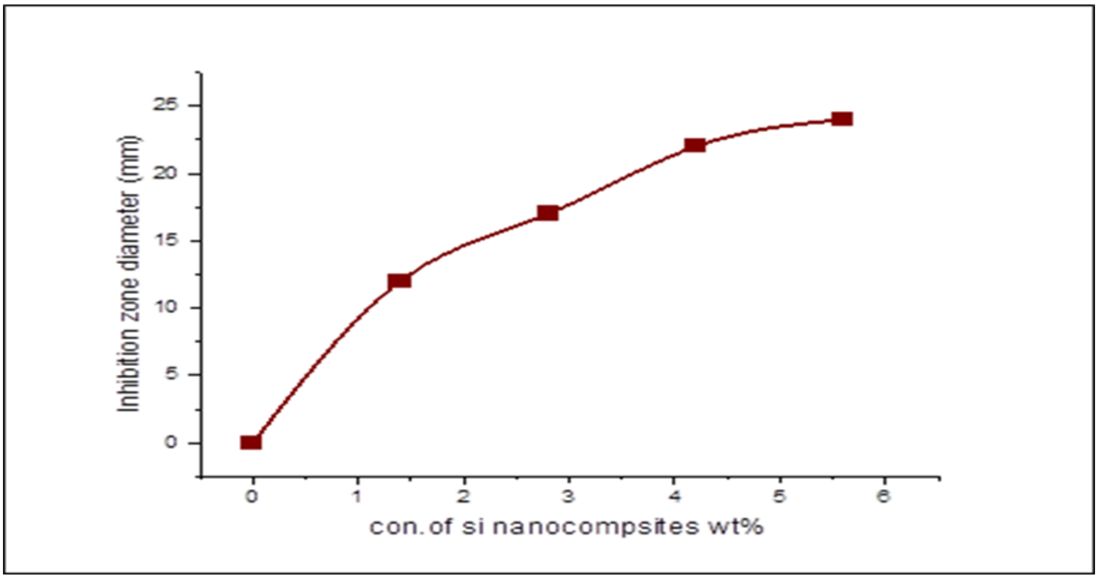

Fig. 11. Inhibition zone diameter of (PMMA-PEO/Si) nanocomposites against Klebsiella pneumoniae.

radicals: superoxide (O_2), hydroxyl (-OH), hydrogen peroxide (H_2O_2), and singlet oxygen (-O_2).

In bacteria, it has the capacity to inflict harm on both DNA and proteins. The production of reactive oxygen species by silicon dioxide may have contributed to the inhibition of the most dangerous microorganisms. Conversely, the nanoparticles included inside the nanocomposites possess negative charges, resulting in an electromagnetic attraction between them and the associated microorganisms. Following the formation of the attraction, the microorganisms will undergo oxidation and ultimately perish [35]. Concerning the nanocomposites consisting of PMMA-PEO/Si, the width of the inhibitory zone is shown in Table 1 [41,42].

CONCLUSION

FTIR measurement indicated the absence of chemical interaction between the silicon nanoparticles and the polymers utilized in the PMMA-PEO/Si nanocomposites. FESEM analysis demonstrated the uniformity of the silicon and PMMA-PEO nanocomposites, indicating that the average grain size diminished with increasing Si concentration. The analysis demonstrated a reduction in the dielectric constant ε› of the samples as the applied electric field intensity increased, a tendency that aligns with the observed patterns of dielectric loss ε››. The augmented frequency improved the alternating current electrical conductivity of the PMMA-PEO/Si nanocomposites. Both dielectric loss and dielectric constant values escalated across all concentration combinations with the augmentation of silicon dioxide content. The antibacterial efficacy of the PMMA-PEO/Si nanocomposites demonstrated that the inhibition zone against Staphylococcus aureus and Klebsiella pneumoniae expanded with higher concentrations of silicon nanoparticles. This illustrates the capabilities of nanoparticles in medical applications, including the eradication and suppression of microorganisms, as well as in electrical and industrial domains.

CONFLICT OF INTEREST

The authors declare that there is no conflict of interests regarding the publication of this manuscript.

REFERENCES

1. Paul DR, Robeson LM. Polymer nanotechnology: Nanocomposites. Polymer. 2008;49(15):3187-3204.
2. Papirer E. The effect of filler shape on the mechanical properties of a reinforced vulcanizate: The SBR-ground asbestos system. Journal of Polymer Science: Polymer Chemistry Edition. 1983;21(9):2833-2836.
3. Moniruzzaman M, Winey KI. Polymer Nanocomposites Containing Carbon Nanotubes. Macromolecules. 2006;39(16):5194-5205.
4. Kadhim MA, Al-Bermany E. Structural and DC-electrical properties of novel PMMA-PVA nanocomposites reinforced with graphene nanosheets. IOP Conference Series: Materials Science and Engineering. 2021;1067(1):012120.
5. Abdulridha AR, Al-Bermany E, Hashim FS, Omran Alkhayatt AH. Synthesis and characterization and pelletization pressure effect on the properties of $Bi_{1.7}Pb_{0.3}Sr_2W_{0.2}Ca_2Cu_3 O_{10+δ}$ superconductor system. Intermetallics. 2020;127:106967.
6. Mohamed Ali T, Padmanathan N, Selladurai S. Effect of nanofiller CeO_2 on structural, conductivity, and dielectric behaviors of plasticized blend nanocomposite polymer electrolyte. Ionics. 2014;21(3):829-840.
7. Al-Bermany E, Qais D, Al-Rubaye S. Graphene Effect on the Mechanical Properties of Poly (Ethylene Oxide)/ Graphene Oxide Nanocomposites Using Ultrasound Technique. Journal of Physics: Conference Series. 2019;1234(1):012011.
8. Abdelamir AI, Al-Bermany E, Hashim FS. Important factors affecting the microstructure and mechanical properties of PEG/GO-based nanographene composites fabricated applying assembly-acoustic method. AIP Conference Proceedings: AIP Publishing; 2020. p. 020110.
9. Vaia RA, Maguire JF. Polymer Nanocomposites with Prescribed Morphology: Going beyond Nanoparticle-Filled Polymers. Chem Mater. 2007;19(11):2736-2751.
10. Haque SR, Boro P, Phukan P, Bhattacharjee S. A comparative study between PANI, PANI/PbS and PANI/PbS/ZnO core/shell quantum dots as chemiresistive sensor for the detection of formaldehyde gas. Journal of Materials Science: Materials in Electronics. 2024;35(30).
11. Kinetic and thermodynamic study of adsorption of an industrial food dye using Iraqi clay. J Popul Ther Clin Pharmacol. 2023;30(5).
12. Cabassi R, Delmonte D, Abbas MM, Abdulridha AR, Gilioli E. The Role of Chemical Substitutions on Bi-2212 Superconductors. Crystals. 2020;10(6):462.
13. Oboudi SF, Al-Habeeb MQ. Gold Nanoparticles Effect on (Bi,Pb)-2223 Superconducting Thin Films. Applied Physics Research. 2016;8(5):64.
14. Abdelrazek EM, Hezma AM, El-khodary A, Elzayat AM. Spectroscopic studies and thermal properties of PCL/PMMA biopolymer blend. Egyptian Journal of Basic and Applied Sciences. 2016;3(1):10-15.
15. Thakur VK, Vennerberg D, Madbouly SA, Kessler MR. Bio-inspired green surface functionalization of PMMA for multifunctional capacitors. RSC Advances. 2014;4(13):6677.
16. Alsaad AM, Ahmad AA, Qattan IA, El-Ali A-R, Fawares SAA, Al-Bataineh QM. Synthesis of Optically Tunable and Thermally Stable PMMA–PVA/CuO NPs Hybrid Nanocomposite Thin Films. Polymers. 2021;13(11):1715.
17. Yang XQ, Lee HS, Hanson L, McBreen J, Okamoto Y. Development of a new plasticizer for poly(ethylene oxide)-based polymer electrolyte and the investigation of their ion-pair dissociation effect. J Power Sources. 1995;54(2):198-204.
18. Azizi Samir MAS, Alloin F, Sanchez J-Y, Dufresne A. Cellulose

nanocrystals reinforced poly(oxyethylene). Polymer. 2004;45(12):4149-4157.
19. Azizi Samir MAS, Chazeau L, Alloin F, Cavaillé JY, Dufresne A, Sanchez JY. POE-based nanocomposite polymer electrolytes reinforced with cellulose whiskers. Electrochimica Acta. 2005;50(19):3897-3903.
20. Storey CJ, Nekovic E, Kaplan A, Theis W, Canham LT. Preserving surface area and porosity during fabrication of silicon aerocrystal particles from anodized wafers. J Porous Mater. 2020;28(2):355-360.
21. Rodriguez I, Shi L, Lu X, Korgel BA, Alvarez-Puebla RA, Meseguer F. Silicon nanoparticles as Raman scattering enhancers. Nanoscale. 2014;6(11):5666-5670.
22. Kuzmin PG, Shafeev GA, Bukin VV, Garnov SV, Farcau C, Carles R, et al. Silicon Nanoparticles Produced by Femtosecond Laser Ablation in Ethanol: Size Control, Structural Characterization, and Optical Properties. The Journal of Physical Chemistry C. 2010;114(36):15266-15273.
23. Zywietz U, Reinhardt C, Evlyukhin AB, Birr T, Chichkov BN. Generation and patterning of Si nanoparticles by femtosecond laser pulses. Appl Phys A. 2013;114(1):45-50.
24. Zywietz U, Evlyukhin AB, Reinhardt C, Chichkov BN. Laser printing of silicon nanoparticles with resonant optical electric and magnetic responses. Nature Communications. 2014;5(1).
25. Maeng S-H, Lee H, Kim S. Synthesis of silicon nanoparticles using a novel reactor with an elongated reaction zone created by coaxially aligned SiH4 gas and a CO2 laser beam. J Nanopart Res. 2021;23(6).
26. Kim S, Hwang C, Park SY, Ko S-J, Park H, Choi WC, et al. High-yield synthesis of single-crystal silicon nanoparticles as anode materials of lithium ion batteries via photosensitizer-assisted laser pyrolysis. J Mater Chem A. 2014;2(42):18070-18075.
27. Mangolini L, Thimsen E, Kortshagen U. High-Yield Plasma Synthesis of Luminescent Silicon Nanocrystals. Nano Lett. 2005;5(4):655-659.
28. Lin N, Han Y, Wang L, Zhou J, Zhou J, Zhu Y, et al. Preparation of Nanocrystalline Silicon from $SiCl_4$ at 200 °C in Molten Salt for High-Performance Anodes for Lithium Ion Batteries. Angew Chem Int Ed. 2015;54(12):3822-3825.
29. Kim H, Seo M, Park MH, Cho J. A Critical Size of Silicon Nano-Anodes for Lithium Rechargeable Batteries. Angew Chem Int Ed. 2010;49(12):2146-2149.
30. Rai A, Prabhune A, Perry CC. Antibiotic mediated synthesis of gold nanoparticles with potent antimicrobial activity and their application in antimicrobial coatings. J Mater Chem. 2010;20(32):6789.
31. Nanocosmetics and Nanomedicines. Springer Berlin Heidelberg; 2011.
32. Sambhy V, MacBride MM, Peterson BR, Sen A. Silver Bromide Nanoparticle/Polymer Composites: Dual Action Tunable Antimicrobial Materials. Journal of the American Chemical Society. 2006;128(30):9798-9808.
33. Sk K, N V, Rb B, Madivalappa S. Structural and optical properties of polyvinyl alcohol/copper oxide (PVA/CuO) nanocomposites. Solid State Commun. 2023;370:115221.
34. Toman MS, Al-nesrawy SH. New Fabrication (PVA-CMC -PbO) Nanocomposites Structural and Electrical Properties. Neuroquantology. 2021;19(4):38-46.
35. Hashim A, Agool IR, Kadhim KJ. Novel of (polymer blend-Fe_3O_4) magnetic nanocomposites: preparation and characterization for thermal energy storage and release, gamma ray shielding, antibacterial activity and humidity sensors applications. Journal of Materials Science: Materials in Electronics. 2018;29(12):10369-10394.
36. Mohammed AJ, Al-nesrawy SH. Nano Ferrite Incorporated Poly (Vinyl Pyrrolidone (PVP) /Poly (Vinyl Alcohol (PVA) Blend: Preparation and Investigation of Structural, Morphological and Optical Properties. Neuroquantology. 2022;20(4):251-258.
37. Fadil OB, Hashim A. Fabrication and Tailored Optical Characteristics of CeO_2/SiO_2 Nanostructures Doped PMMA for Electronics and Optics Fields. Silicon. 2022;14(15):9845-9852.
38. Abdullah OG, Saleem SA. Effect of Copper Sulfide Nanoparticles on the Optical and Electrical Behavior of Poly(vinyl alcohol) Films. J Electron Mater. 2016;45(11):5910-5920.
39. Rajesh K, Crasta V, Rithin Kumar NB, Shetty G, Rekha PD. Structural, optical, mechanical and dielectric properties of titanium dioxide doped PVA/PVP nanocomposite. Journal of Polymer Research. 2019;26(4).
40. Size-Controlled $SrTiO_3$ Nanoparticles Photodecorated with Pd Cocatalysts for Photocatalytic Organic Dye Degradation. American Chemical Society (ACS). http://dx.doi.org/10.1021/acsanm.0c01086.s001
41. Asab G, Zereffa EA, Abdo Seghne T. Synthesis of Silica-Coated Fe_3O_4 Nanoparticles by Microemulsion Method: Characterization and Evaluation of Antimicrobial Activity. International Journal of Biomaterials. 2020;2020:1-11.
42. Mohammed RM. Effect of Antimony Oxide Nanoparticles on Structural, Optical and AC Electrical Properties of (PEO-PVA) Blend for Antibacterial Applications. International Journal of Emerging Trends in Engineering Research. 2020;8(8):4726-4738.